



# Florigen-like protein OsFTL1 promotes flowering without essential florigens Hd3a and RFT1 in rice

Shaobo Wei<sup>1,2†</sup>, Long Cheng<sup>3†</sup>, Hongge Qian<sup>4†</sup>, Xia Li<sup>1,2</sup>, Lianguang Shang<sup>4</sup>, Yujie Zhou<sup>1</sup>, Xiangyuan Ye<sup>1</sup>, Yupeng Zhou<sup>1</sup>, Yuan Gao<sup>1</sup>, Lin Cheng<sup>1</sup>, Chen Xie<sup>1</sup>, Qingwen Yang<sup>1,2</sup>, Qian Qian<sup>1\*</sup> and Wenbin Zhou<sup>1,2\*</sup>

1. Institute of Crop Sciences, Chinese Academy of Agricultural Sciences, Beijing 100081, China

2. State Key Laboratory of Crop Gene Resources and Breeding, Institute of Crop Sciences, Chinese Academy of Agricultural Sciences, Beijing 100081, China

3. MOA Key Laboratory of Crop Ecophysiology and Farming System in the Middle Reaches of the Yangtze River, College of Plant Science and Technology, Huazhong Agricultural University, Wuhan 430070, China

4. Lingnan Laboratory of Modern Agriculture, Genome Analysis Laboratory of the Ministry of Agriculture, Agricultural Genomics Institute at Shenzhen, Chinese Academy of Agricultural Sciences, Shenzhen 518124, China

<sup>†</sup>These authors contributed equally to this work.

\*Correspondences: Qian Qian ([qianqian@caas.cn](mailto:qianqian@caas.cn)); Wenbin Zhou ([zhouwenbin@caas.cn](mailto:zhouwenbin@caas.cn), Dr. Zhou is fully responsible for the distributions of all materials associated with this article)



Shaobo Wei



Wenbin Zhou

## ABSTRACT

Flowering time is a critical agronomic trait in rice, directly influencing grain yield and adaptability to specific planting regions and seasons. Florigens, including FLOWERING LOCUS T (FT) proteins Hd3a (OsFTL2) and RFT1 (OsFTL3), play central roles in transmitting flowering signals through rice's photoperiod regulatory network. While Hd3a and RFT1 have been extensively studied, the functions and interactions of other FT-like proteins remain unclear, limiting advancements in breeding strategies for early-maturing rice varieties. Here, we demonstrate that the florigen-like protein OsFTL1 forms a florigen activation complex (FAC) and promotes flowering under both short-day and long-day con-

ditions. OsFTL1 localizes to the nucleus and cytoplasm, with predominant expression in the shoot base, facilitating its mobilization to the shoot apical meristem (SAM) to initiate flowering. Overexpression of OsFTL1 (OsFTL1-OE) in leaves or shoot bases significantly accelerates flowering and alters plant architecture. In the nucleus, OsFTL1 interacts with GF14c and OsFD1 to form an FAC, activating OsMADS14 and OsMADS15 expression to drive flowering. Markedly, OsFTL1-OE plants deficient in Hd3a and RFT1 exhibited earlier flowering compared with wild-type plants, indicating that OsFTL1 can independently promote flowering. Furthermore, haplotype analysis identified OsFTL1-Hap3, a beneficial variant associated with early flowering and comparable grain yields. These findings revealed that OsFTL1 can substitute for Hd3a and RFT1 in FAC formation, promoting flowering across photoperiods, and highlighting its potential application in breeding early-maturing, high-yield rice varieties suitable for diverse environments.

Keywords: beneficial haplotype, florigen, flowering time, OsFTL1, rice

Wei, S., Cheng, L., Qian, H., Li, X., Shang, L., Zhou, Y., Ye, X., Zhou, Y., Gao, Y., Cheng, L., et al. (2025). Florigen-like protein OsFTL1 promotes flowering without essential florigens Hd3a and RFT1 in rice. *J. Integr. Plant Biol.* **00**: 1–16.

## INTRODUCTION

The transition from vegetative to reproductive growth—flowering—is a pivotal phase in crop development,

directly affecting yield and regional adaptability. In rice, flowering time is determined by a complex interplay of photoperiod sensitivity, temperature sensitivity, and vegetative growth duration, each of them shaping yield outcomes

## OsFTL1 promotes flowering without essential florigens

across agricultural zones (Cho et al., 2017; Vicentini et al., 2023). Breeding strategies for high-yield, early-maturing rice varieties aim to optimize these traits to ensure consistent production across varying environments.

Photoperiod sensitivity plays a dominant role in controlling rice flowering. As a facultative short-day plant, rice employs two distinct molecular regulatory networks under short-day and long-day conditions. The *Hd1-Hd3a/RFT1* module predominantly governs flowering under short days, while the *Hd1/Ghd7/DTH8-Ehd1-Hd3a/RFT1* pathway regulates flowering under long days (Sun et al., 2014; Zong et al., 2021). The photoperiodic controlled pathway of flowering regulation in rice has been defined (Zhou et al., 2021), including the critical nodes *Hd1* and *Ehd1* modulating the expression of florigen genes.

*Hd1*, homologous to *Arabidopsis*' *CONSTANS* (*CO*), promotes flowering under short-day conditions and represses it under long-day conditions (Yano et al., 2000). In addition, *Ehd1*, a B-type response regulator, activates florigen gene expression irrespective of day length (Doi et al., 2004; Zhao et al., 2015). Additional MADS-box transcription factors *OsMADS50* and *OsMADS51* act upstream of flowering activators *OsMADS14*, *OsMADS15*, and *Hd3a* (Lee et al., 2004), while *OsMADS51* acts upstream of the major flowering activators *Ehd1*, *OsMADS14*, and *Hd3a* to promote rice flowering (Kim et al., 2007). A network of other genes, including *Ehd2*, *OsCOL4*, *PhyB*, and *OsRR1*, participates in flowering signal transduction under short-day or long-day conditions (Matsubara et al., 2008; Lee et al., 2010; Cho et al., 2016; Sheng et al., 2016; Zhou et al., 2021). In addition, in rice, several pleiotropic genes, such as *Ghd7*, *DTH8*, and *Ef-cd*, that affect grain yield, also control flowering time. For instance, *Ghd7* and *DTH8* delay flowering time by producing a repression complex with *Hd1* under long-day conditions, and *Ef-cd* promotes flowering by encoding a long noncoding RNA to regulate the histone methylation levels to promote the expression of *OsSOC1* (Xue et al., 2008; Wei et al., 2010; Fang et al., 2019a; Zong et al., 2021). Collectively, these genes form a complex flowering time regulatory network that transmits flowering signals to the florigen genes *Hd3a* and *RFT1*.

Florigen, a key regulator of flowering, belongs to the phosphatidylethanolamine-binding protein (PEBPs) family and translocates from the leaf to the shoot apex to induce floral initiation by transmitting flowering signals to downstream regulators (Jin et al., 2021). In rice, there are 13 *FT-like* (*FTL*) genes. Two of these, *Hd3a* (*OsFTL2*) and *RFT1* (*OsFTL3*), homologs of *Arabidopsis* *FLOWERING LOCUS T* (*FT*), promote rice flowering under short-day and long-day conditions, respectively (Kojima et al., 2002; Komiya et al., 2008; Peng et al., 2021). Under short-day conditions, *Hd3a* interacts with FT-INTERACTING PROTEIN 9 (*OsFTIP9*) to facilitate *Hd3a* transport from companion cells to sieve elements (Zhang et al., 2022); under long-day conditions, *RFT1* interacts with FT-INTERACTING PROTEIN 1 (*OsFTIP1*) to facilitate the transport of *RFT1* from companion cells to sieve

elements (Song et al., 2017). The interactions between these proteins were enhanced by tetratricopeptide repeat protein 075 (*OsTPR075*), promoting the transport of florigens from rice leaves to the shoot apical meristem (SAM) (Zhang et al., 2022). Florigens (*Hd3a* and *RFT1*), 14-3-3 proteins (*GF14b* and *GF14c*), and the transcription factor *OsFD1* form the florigen activation complex (FAC) in the nucleus in rice SAM, to activate the expression of *OsMADS14* and *OsMADS15* to promote flowering (Taoka et al., 2011). In contrast, the rice florigen-like protein *OsFTL12* is a flowering inhibitor, competing with *Hd3a* for binding to *GF14b* to form a flowering repression complex (FRC) (Zheng et al., 2023). The flowering time of *osftl4* mutants is 5.8–9.6 d earlier than wild-type (WT) (Gu et al., 2022). Also, overexpression of *OsFTL10* shortens flowering time by approximately 14 d compared with WT (Fang et al., 2019b). Despite detailed characterizations of individual florigens and florigen-like proteins on flowering time in rice, the interactions among florigens and florigen-like proteins and their influence on flowering time are poorly understood, limiting the capacity of breeders to control flowering time using *FTL* alleles.

In addition to *Hd3a* and *RFT1*, which are expressed in leaves and migrate to SAM to drive floral commitment, *FLOWERING LOCUS T-LIKE 1* (*OsFTL1*; *LOC\_Os01g11940*) is a florigen-like protein that is not typically expressed in leaves. Functionally, *OsFTL1* is similar to reported florigens and contributes to the vegetative to inflorescence meristem transition. It has been shown that *OsFTL1* collaborates with *Hd3a* and *RFT1* during floral induction (Giaume et al., 2023). However, the details regarding *OsFTL1*-interacting proteins and their influence on flowering time and grain yield are largely unknown.

Here, we uncover that *OsFTL1* promotes flowering by forming a FAC with *GF14c* and *OsFD1* under both short-day and long-day conditions. Importantly, *OsFTL1* is capable of inducing flowering independently of *Hd3a* and *RFT1*. Haplotype analysis revealed that *OsFTL1-Hap3* confers early flowering and stable grain yield, underscoring its potential utility in breeding early-maturing rice varieties adaptable to diverse environments.

## RESULTS

### *OsFTL1* regulates flowering time and yield-related traits in rice

Previous studies have demonstrated that *OsDREB1C* promotes flowering in rice by binding to an exon of *OsFTL1*, thereby activating its expression in *OsDREB1C*-overexpressing plants (Wei et al., 2022). Fine-mapping analyses also identified *OsFTL1* as a candidate gene that influences flowering time (Wang et al., 2011; Liu et al., 2022). However, its precise regulatory mechanisms remain unclear (Izawa et al., 2002; Giaume et al., 2023; Wei et al., 2024; Zhao et al., 2024).

To investigate *OsFTL1* function, we developed *OsFTL1*-overexpressing (*OsFTL1*-OE) rice lines using the maize

ubiquitin (UBI) promoter on the *Oryza sativa* cv. Nipponbare background. Three lines were selected for further analysis based on hygromycin resistance and *OsFTL1* expression levels measured by quantitative real-time-polymerase chain reaction (qRT-PCR) (Figure S1). Field trials in Beijing over 2 consecutive years consistently showed earlier flowering in *OsFTL1*-OE plants compared with WT in 2021 (51.2 vs. 116.25 d, respectively) (Figure 1A, B) and in 2022 (51.6d vs. 103.2 d, respectively) (Table S1).

Early flowering in *OsFTL1*-OE plants led to reduced agronomic traits, including grain number per panicle, grain yield per plant, plant height, and aboveground dry weight, despite increases in panicle number and 1,000-grain weight (Figure 1C–H; Table S1). Measurements of grain dimensions revealed that *OsFTL1*-OE grains were longer and thicker than WT, although grain thickness increases in *OsFTL1*-OE2/3 were not significant, and grain width remained unchanged (Figure S2A, B).

Additionally, *OsFTL1*-OE plants exhibited dwarfism, with fewer stem nodes, shorter stems, and reduced stem diameter compared with WT (Figure S3A–C). We also generated *osftl1* mutants using CRISPR–Cas9 technology and identified three lines (*osftl1*-1/2/3) with mutated *OsFTL1* proteins. In autumn 2024 in Beijing, these mutants exhibited delayed flowering (104.3–107.7 d) compared with WT (Nipponbare, 99.5 d) (Figure 2). Collectively, these findings established

*OsFTL1* promotes flowering without essential florigens

*OsFTL1* as a key activator of flowering time and a regulator of yield-related traits in rice.

Under both short-day and long-day conditions, *OsFTL1*-OE plants flowered significantly earlier than WT, with flowering times under long-day conditions (38–42 d) matching those under short-day conditions, indicating photoperiod insensitivity (Figure S4A–C). At flowering, *OsFTL1*-OE plants had significantly fewer leaves than WT, suggesting that earlier flowering resulted from altered developmental processes rather than accelerated growth rates (Figure S4D, E).

### *OsFTL1* expression patterns and induction by short-day conditions

To characterize *OsFTL1* molecular functions, we performed a phylogenetic analysis of 13 FT-like proteins in rice, showing that *OsFTL1* was closely related to Hd3a and RFT1. Among Poaceae crop plants, *OsFTL1* (XP\_015611892), *ZmFTL1* (NP\_001106251.1), and *TaFTL1* (XP\_044347923.1) shared the same branch of the phylogenetic tree (Figure 3A). Expression profiling revealed a gradual increase in *OsFTL1* expression in leaves during development, with peak expression at 90 d after sowing (Figure 3B). Tissue-specific analysis showed that *OsFTL1* was predominantly expressed in stems, leaves, and panicles at the heading stage, confirmed by GUS staining (Figure 3C, D). Notably, GUS staining of 90-d leaves uncovered specific expression of *OsFTL1* in

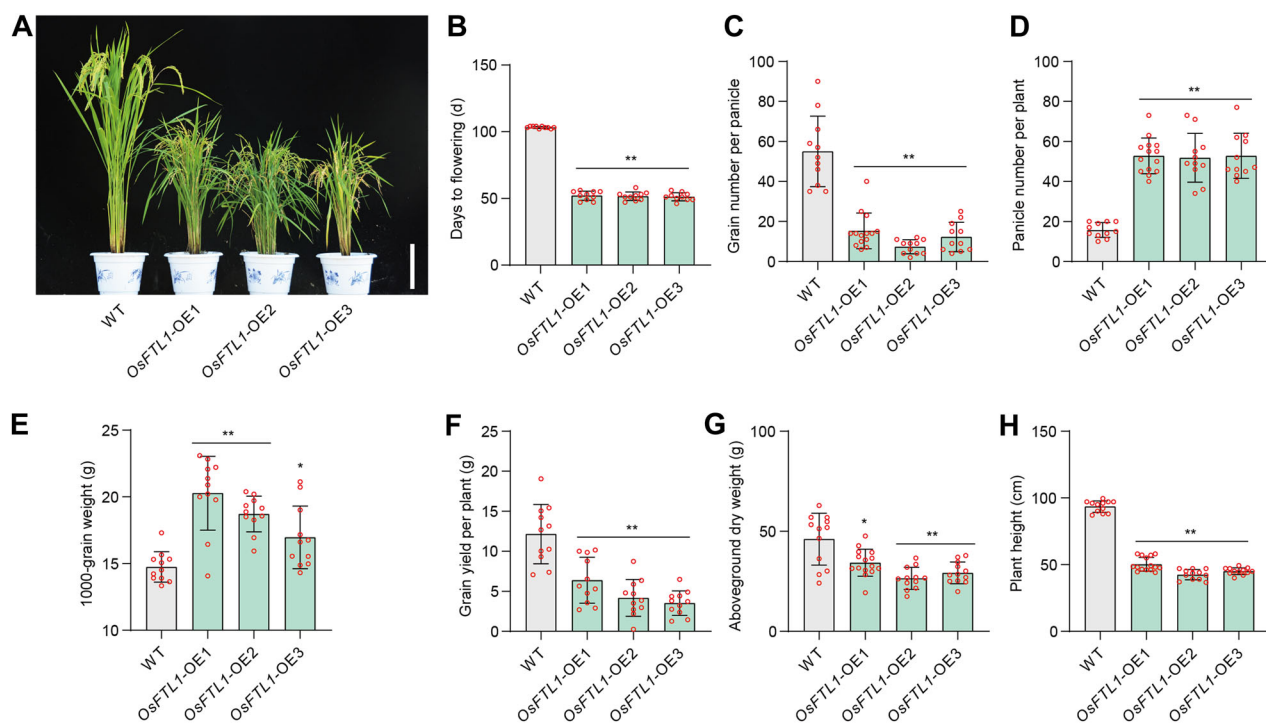


**Figure 1. Overexpression of *OsFTL1* promotes rice flowering and regulates yield-related traits**

(A) Phenotypic comparison of *OsFTL1*-OE and wild-type (WT) (Nipponbare) plants grown in Beijing in 2022. Scale bar: 20 cm. (B–H) Data for flowering time, grain number per panicle, panicle number per plant, 1,000-grain weight, grain yield per plant, aboveground dry weight, and plant height collected in Beijing in 2022. Values represent means  $\pm$  SD ( $n \geq 10$  plants). \* and \*\* indicate statistically significant differences compared with WT at  $P < 0.05$  and  $P < 0.01$ , respectively, based on Student's *t*-tests.

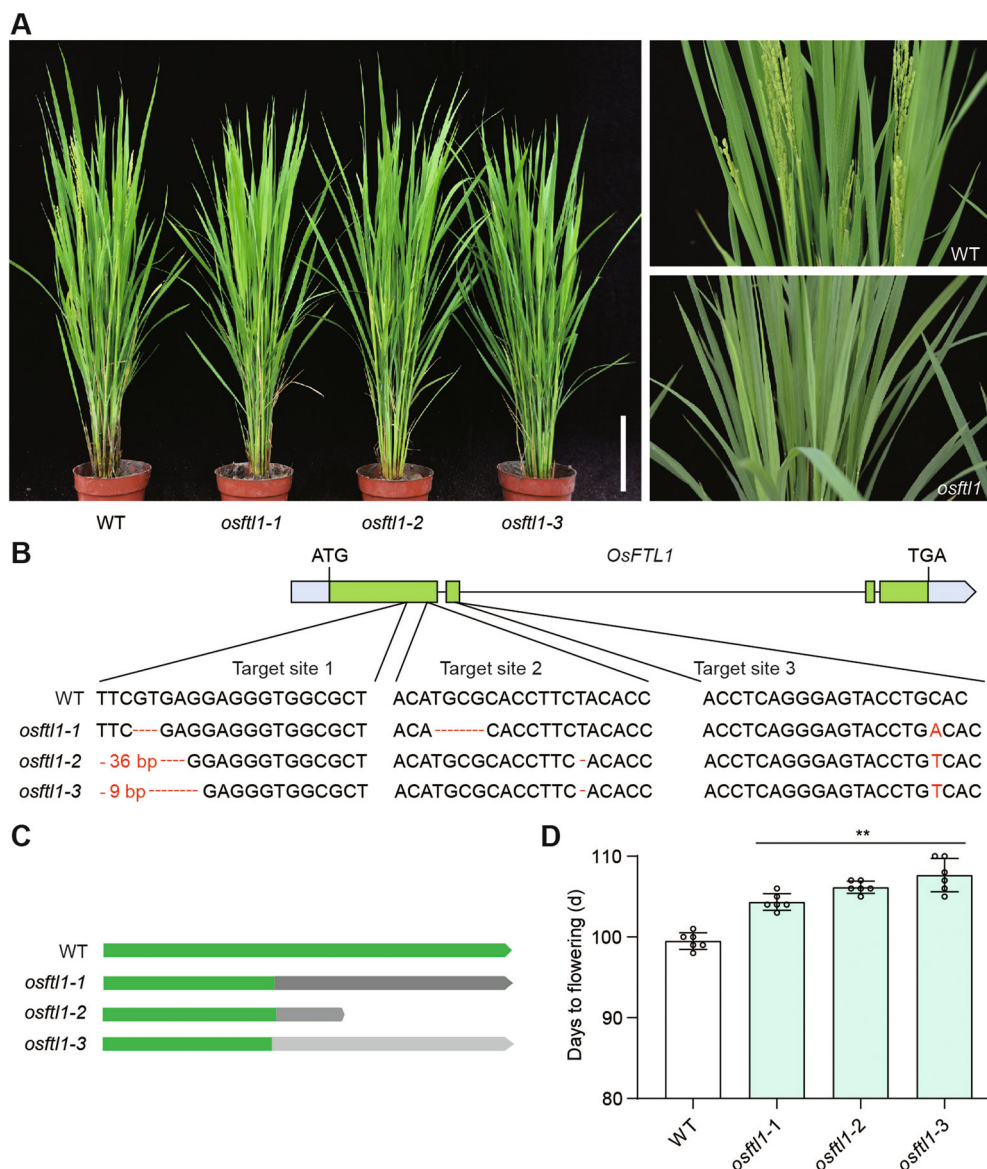


**Figure 2. Flowering time of *osftl1* mutants in Beijing in 2024**

**(A)** Phenotype of *osftl1* mutants and wild-type (WT) plants grown in Beijing in 2024. Scale bar: 20 cm. **(B)** Genotype of *osftl1* mutants and WT plants. **(C)** Comparison of *OsFTL1* protein sequences between WT and *osftl1* mutants. Green bars represent sequences identical to *OsFTL1*; gray bars indicate mutant amino acids. **(D)** Flowering time of *osftl1* mutants and WT plants in Beijing in 2024. Data represent means ± SD ( $n = 6$  biological replicates). \* and \*\* indicate statistically significant differences compared with WT at  $P < 0.05$  and  $P < 0.01$ , respectively, based on Student's *t*-tests.

the phloem of vascular bundles (Figure 3D); however, in 30-d seedlings, *OsFTL1* was expressed in the shoot base and leaf sheath (Figure 3E). This expression pattern in *OsFTL1* differed from *Hd3a* and *RFT1*, which are expressed mainly in leaves (Tamaki et al., 2007; Komiya et al., 2009), and suggested that *OsFTL1* functions in the meristem compared with typical florigens.

At the protein level, ectopic expression of *pUBI::OsFTL1-GFP* showed that *OsFTL1-GFP* was localized to the nucleus and cytoplasm of leaf sheath and root cells, consistent with the subcellular localization of *OsFTL1-GFP* in rice protoplasts (Figure 3F, G). These findings indicated that *OsFTL1* is a

unique FT-like protein with a specific expression pattern in the shoot base.

To evaluate the response of *OsFTL1* expression to photoperiod, we treated Nipponbare (WT), *pOsFTL1::GUS*, and *pOsFTL1::OsFTL1-GFP* plants with long-day (16 h light/8 h dark) and short-day (8 h light/16 h dark) exposures. *OsFTL1* expression levels in the shoot base of 3-week Nipponbare plants were higher under short-day conditions than long-day conditions; similar findings were obtained by GUS staining in *pOsFTL1::GUS* plants (Figure S5A, B). In *pOsFTL1::OsFTL1-GFP* plants, *OsFTL1-GFP* protein was detected across various tissues, including the shoot base, leaf sheath, and

glume, while the levels of OsFTL1-GFP present in these tissues were higher under short-day versus long-day conditions, especially in the shoot base (Figure S5C). The specific expression of OsFTL1-GFP protein in SAM was also confirmed in 30-d-old *proOsFTL1::OsFTL1-GFP* plants by confocal microscopy (Figure S6). These findings supported

the specific expression of *OsFTL1* in the shoot base, indicating that short-day conditions induced *OsFTL1* expression.

Given the functional similarities and close phylogenetic relationship between *OsFTL1*, and *Hd3a/RFT1* (Figure 3A), we examined their roles in flowering across rice varieties.

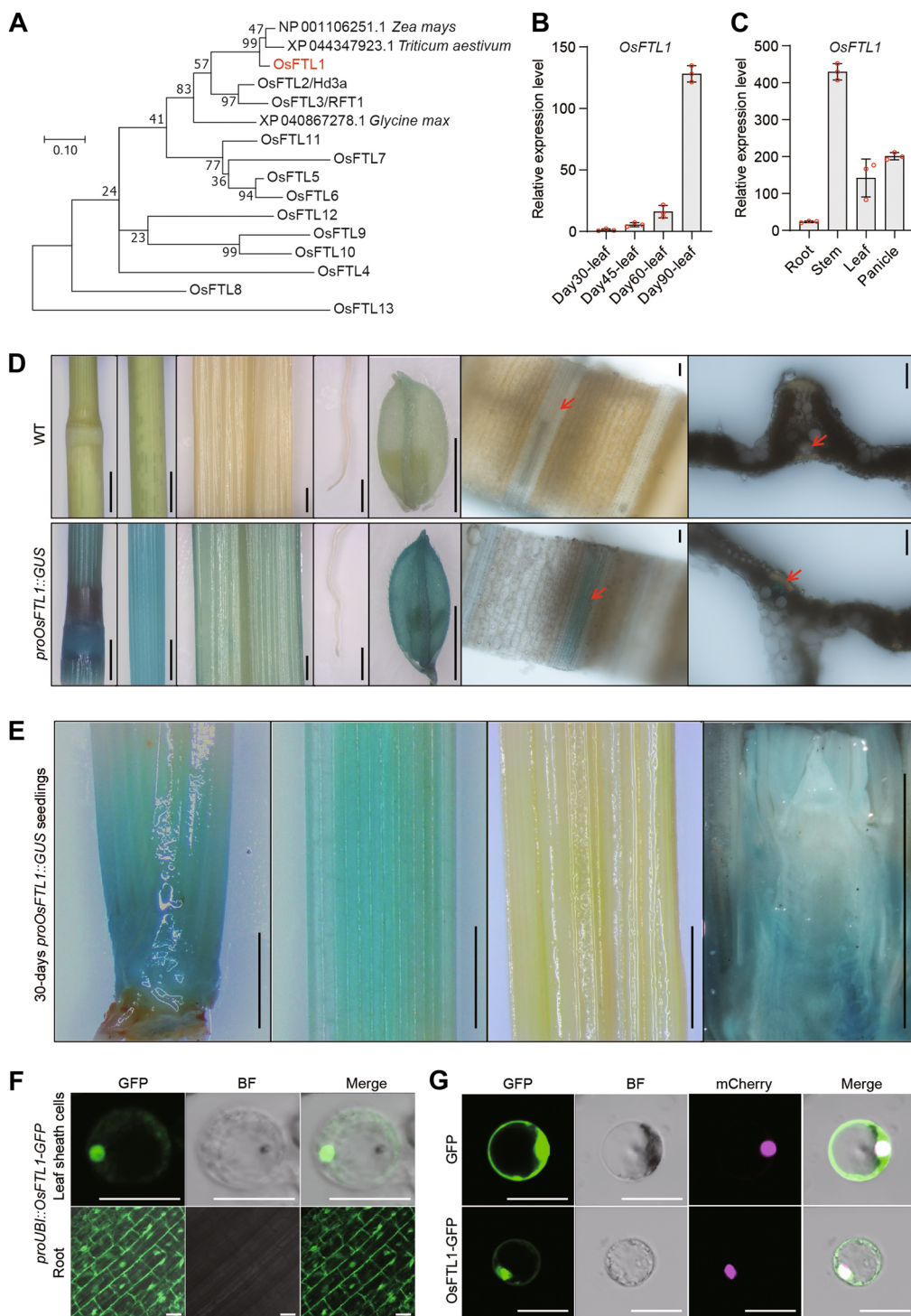


FIGURE 3 Continued.

## OsFTL1 promotes flowering without essential florigens

Quantitative RT-PCR analysis revealed higher *RFT1* expression compared with *OsFTL1* and *Hd3a* during vegetative growth in both *japonica* variety Nipponbare and *indica* variety 9311 under natural long-day conditions in Beijing (Figure S7A, B), confirming *RFT1* as the primary promoter of flowering under these conditions (Komiya et al., 2009; Peng et al., 2021). In contrast, under natural short-day conditions in Sanya, *OsFTL1* expression surpassed that of *Hd3a* and *RFT1* throughout development, highlighting its role in flowering regulation under short-day conditions (Figure S7C, D).

### OsFTL1 forms a FAC with GF14c and OsFD1 to promote flowering

To investigate the molecular mechanism by which *OsFTL1* regulates flowering, we conducted immunoprecipitation-mass spectrometry (IP-MS) using 4-week-old seedlings of Nipponbare (WT) and *pUBI::OsFTL1-GFP* transgenic plants. This analysis identified 24 candidate *OsFTL1*-interacting proteins, including GF14c, a 14-3-3 protein known for its role in flowering time regulation (Taoka et al., 2011) (Table S2). Subsequent experiments confirmed the interaction between *OsFTL1* and GF14c in the cytoplasm, as demonstrated by co-immunoprecipitation (co-IP), pull-down and bimolecular fluorescence complementation (BiFC) assays (Figures 4A–C, S8).

Furthermore, BiFC and co-localization assays conducted in *Nicotiana benthamiana* leaf cells and rice protoplasts revealed that the transcription factor *OsFD1*—another component of the FAC—facilitated the nuclear translocation of *OsFTL1* and GF14c (Figure 4C, D). Transactivation assays demonstrated that the FAC comprising *OsFTL1*, GF14c, and *OsFD1* activated the expression of the flowering regulators *OsMADS14* and *OsMADS15* (Figure 4E–G). Supporting these findings, qRT-PCR and RNA-seq analyses showed significantly increased *OsMADS14* and *OsMADS15* transcript levels in *OsFTL1*-OE plants compared with WT (Figures 4H, I, S9). Together, these results established the fact that *OsFTL1* forms a FAC with GF14c and *OsFD1* to promote flowering by upregulating *OsMADS14* and *OsMADS15*.

### OsFTL1 promotes flowering independently of *Hd3a* and *RFT1*

The mobile signals *Hd3a* and *RFT1*, expressed in the leaf blade, are known to translocate to the SAM to promote

flowering in rice (Tamaki et al., 2007; Komiya et al., 2009). To determine whether *OsFTL1* can translocate among different tissues in rice, we developed *OsFTL1* transgenic rice using its native promoter in Nipponbare (*pOsFTL1::OsFTL1-GFP*) and the leaf-specific *RFT1* promoter in Xiushui134 (*pRFT1::OsFTL1*) (Komiya et al., 2008). Based on the tissue-specific expression of *OsFTL1* in the shoot base and *RFT1* in the leaf blade, we obtained homozygous plants of five *pOsFTL1::OsFTL1-GFP* lines and three *pRFT1::OsFTL1* lines by evaluating the *OsFTL1* expression levels in shoot base and leaves, respectively. In Beijing, the flowering time of *pOsFTL1::OsFTL1-GFP* plants (51.8–93.75 d) was earlier than Nipponbare (WT) (117.25 d), similar to the early-flowering phenotype of *OsFTL1*-OE plants (Figures 1A, B, 5A, C). Similarly, in Sanya, *pRFT1::OsFTL1* plants flowered earlier (59.8–64.7 d) than Xiushui134 (74.5 d) (Figure 5B, D). These findings indicated that leaf-expressed *OsFTL1* can act as a mobile signal translocating to the SAM to promote flowering.

Previous studies have found that *hd3a* and *rft1* double-knockout plants fail to flower for up to 300 d, underscoring the critical role of these genes in rice flowering (Komiya et al., 2008). Consistent with these findings, we observed no flowering in *hd3a-rft1* double-knockout plants during the entire growth period (Figure S10A–D). To investigate whether *OsFTL1* could compensate for the absence of *Hd3a* and *RFT1*, we used CRISPR–Cas9 technology to generate *hd3a-rft1* double knockouts in *OsFTL1*-OE1 plants, resulting in eight independent *OsFTL1*-OE1<sup>*hd3a-rft1*</sup> lines. Among these, three homozygous lines were confirmed by qRT-PCR and DNA sequencing (Figure 6A, B) and subjected to further analysis.

The flowering time of these homozygous *OsFTL1*-OE1<sup>*hd3a-rft1*</sup> lines (66–72 d) was later than *OsFTL1*-OE1 (57.5 d) but earlier than Nipponbare (WT) plants (83 d) (Figure 6C, D). This suggested that *OsFTL1* could promote flowering even in the absence of the essential florigens *Hd3a* and *RFT1*, probably functioning as a downstream activator in the flowering regulatory network (Giaume et al., 2023).

### Natural variations and domestication of *OsFTL1*

To explore the potential of *OsFTL1* in breeding early-maturing rice varieties, we conducted a haplotype analysis of *OsFTL1* using 153 rice micro-core germplasm accessions. This

### Figure 3. Phylogenetic analysis, expression pattern and subcellular localization of *OsFTL1*

(A) Phylogenetic tree of 13 rice *FTL* proteins and homologs of *OsFTL1* from *Zea mays*, *Triticum aestivum*, and *Glycine max*, constructed using the maximum likelihood algorithm. Numbers at the nodes denote the percentage of 1,000 bootstraps, and the scale bar represents the average number of amino acid substitutions per site. Accession numbers: (*OsFTL1*, LOC\_Os01g11940), (*OsFTL2*, LOC\_Os06g06320), (*OsFTL3*, LOC\_Os06g06300), (*OsFTL4*, LOC\_Os09g33850), (*OsFTL5*, LOC\_Os02g39064), (*OsFTL6*, LOC\_Os04g41130), (*OsFTL7*, LOC\_Os12g13030), (*OsFTL8*, LOC\_Os01g10590), (*OsFTL9*, LOC\_Os01g54490), (*OsFTL10*, LOC\_Os05g44180), (*OsFTL11*, LOC\_Os11g18870), (*OsFTL12*, LOC\_Os06g35940), (*OsFTL13*, LOC\_Os02g13830), (*Oryza sativa*, XP\_015611892) (*Zea mays*, NP\_001106251.1), (*Triticum aestivum*, XP\_044347923.1), (*Glycine max*, XP\_040867278.1). (B) Relative expression levels of *OsFTL1* in Nipponbare leaves at 30, 45, 60, and 90 d after sowing. (C) Relative expression levels of *OsFTL1* in roots, stems, leaves, and panicles of Nipponbare at the heading stage. Data represent means  $\pm$  SD ( $n = 3$  biological replicates). (D) GUS staining in various tissues of the Nipponbare and *pOsFTL1::GUS* plants at the heading stage. Scale bars, 100  $\mu$ m. (E) GUS staining in various tissues of 30-d *pOsFTL1::GUS* seedlings. Scale bars, 3 mm. Subcellular localization of *OsFTL1* in the leaf and root of *pOsFTL1::OsFTL1-GFP* plants (F) and rice protoplasts (G). Scale bars, 20  $\mu$ m. BF, Bright field. mCherry, Ghd7-mCherry as a marker of the nucleus.

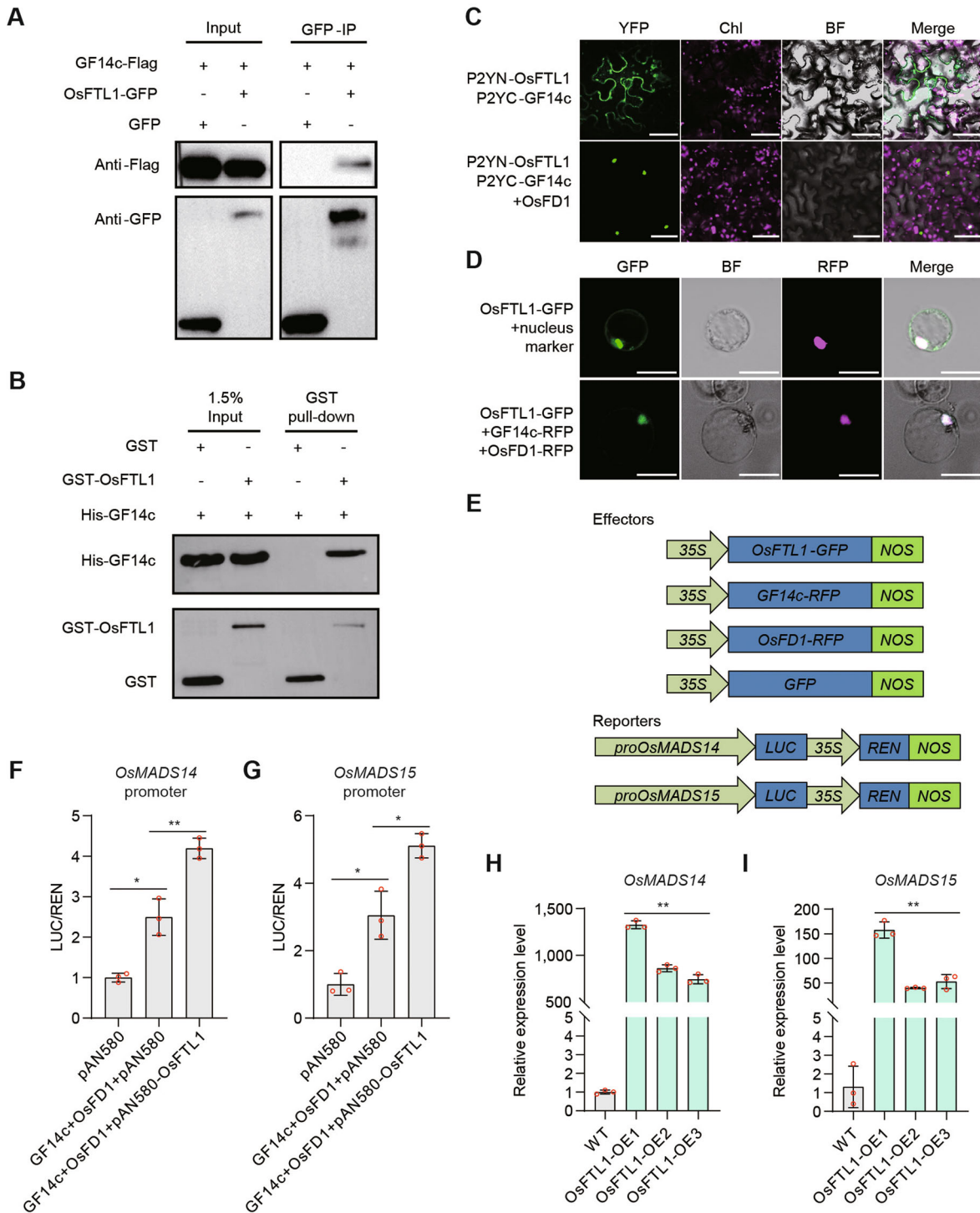


**Figure 4. OsFTL1 forms a florigen activation complex (FAC) with GF14c and OsFD1 in the nucleus to activate the expression of OsMADS14 and OsMADS15**

(A) Co-immunoprecipitation experiments, (B) pull-down, and (C) bimolecular fluorescence complementation (BiFC) assays confirm the interaction of OsFTL1 and GF14c. (C) OsFD1 drives OsFTL1 and GF14c into the nucleus in BiFC assay, scale bars, 50  $\mu$ m. (D) Co-localization of OsFTL1, GF14c, and OsFD1, nucleus marker Ghd7-RFP, scale bars, 20  $\mu$ m. (E) Schematic diagrams of dual-luciferase reporters and effector constructs. (F, G) Luciferase (LUC) reporters driven by *pOsMADS14* and *pOsMADS15* co-transformed with different effectors as indicated. Equal concentrations of effectors or reporters were co-transformed into rice protoplast cells to assess the activities of firefly luciferase (LUC) and Renilla luciferase (REN). Luciferase/Renilla activity shown relative to the empty vector control (set to 1) ( $n = 3$  biological replicates). The expression level of *OsMADS14* (H) and *OsMADS15* (I) in *OsFTL1*-OE and wild-type (WT) plants ( $n = 3$  biological replicates). Data are presented as means  $\pm$  SD. \* and \*\* represent statistically significant differences compared with WT at  $P < 0.05$  and  $P < 0.01$ , respectively, based on Student's *t*-tests.

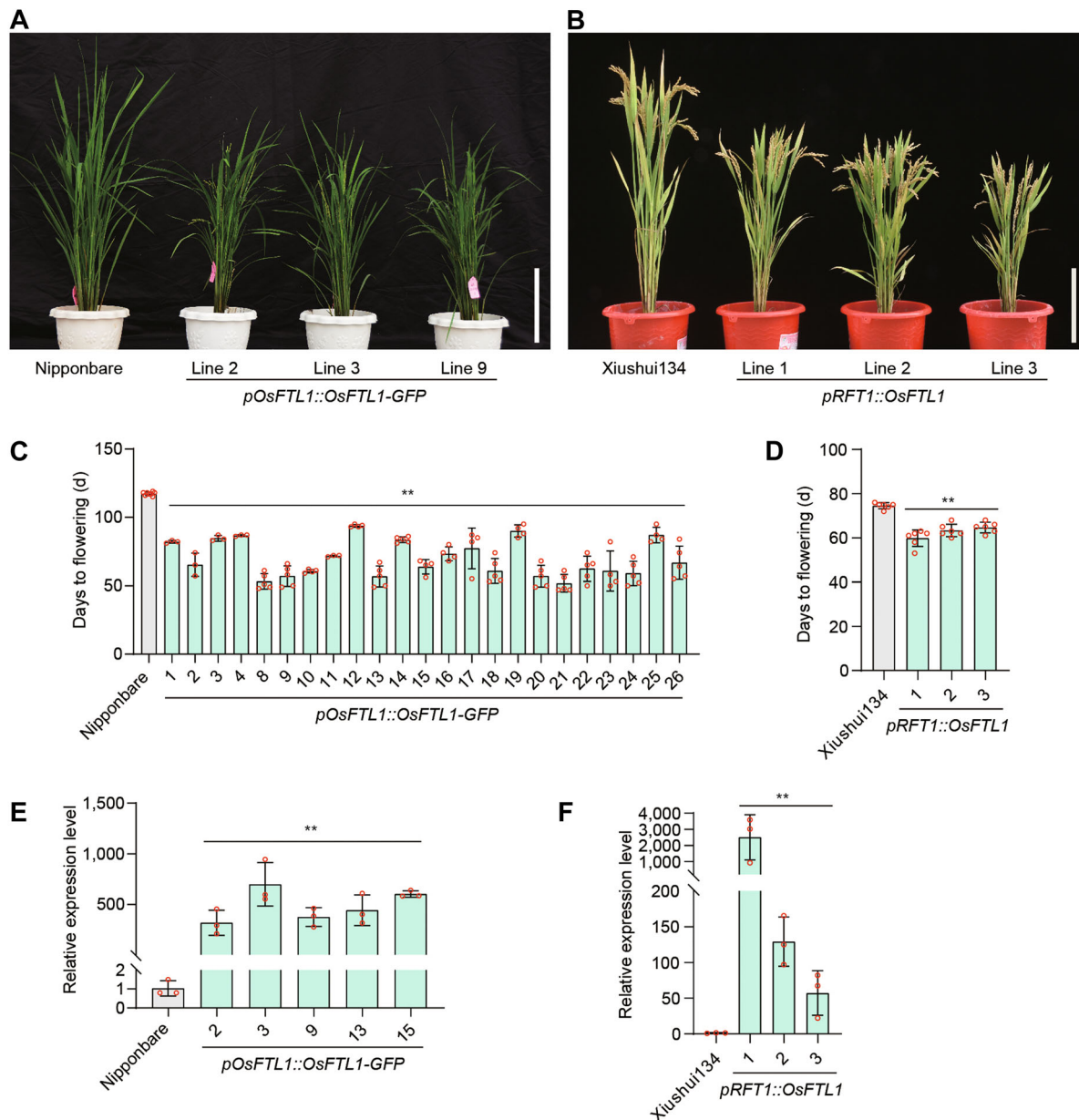


**Figure 5. Overexpression of *OsFTL1* in leaves promotes flowering**

(A) Flowering phenotype of Nipponbare and *pOsFTL1::OsFTL1-GFP* plants in Beijing in 2024, scale bar, 20 cm. (B) Flowering phenotype of Xiushui134 and *pRFT1::OsFTL1* plants in Sanya in 2024, scale bar, 20 cm. (C) Days to flowering in Nipponbare and *pOsFTL1::OsFTL1-GFP* plants in Beijing in 2023 ( $n > 3$  biological replicates). (D) Days to flowering of Xiushui134 and *pRFT1::OsFTL1* plants in Sanya in 2024 ( $n = 6$  biological replicates). (E) Quantitative real-time-polymerase chain reaction (qRT-PCR) analysis of *OsFTL1* expression levels in the shoot base of *pOsFTL1::OsFTL1-GFP* plants and wild-type (WT) ( $n = 3$  biological replicates). (F) Quantitative RT-PCR analysis of *OsFTL1* expression levels in the leaves of *pRFT1::OsFTL1* plants and Xiushui134 ( $n = 3$  biological replicates). Expression levels were normalized to that of *OsActin* (*LOC\_Os03g50885*). \* and \*\* represent statistically significant differences compared with Nipponbare and Xiushui134 at  $P < 0.05$  and  $P < 0.01$ , respectively, based on Student's *t*-tests.

analysis identified five main haplotypes with variations in promoter, exonic, and intronic sequences (Figure 7A). Among these, *OsFTL1-Hap3* emerged as an elite haplotype associated with earlier flowering, specifically within the *indica* subspecies (Figure 7B–D).

Within the promoter of *OsFTL1-Hap3*, four candidate functional variation sites were identified:  $-1,943$  T/C,  $-1,471$  C/CT,  $-1,023$  TAATA/T, and  $-734$  G/A. Notably, grain yield

per plant in *OsFTL1-Hap3* varieties was comparable with other haplotypes, indicating that the early-flowering trait conferred by *OsFTL1-Hap3* did not compromise yield (Figure 7E, F). Additionally, varieties possessing *OsFTL1-Hap3* (e.g., QC55, QC95, QC97, QC163, and QC186) exhibited higher *OsFTL1* expression levels and earlier flowering compared with varieties with other haplotypes (e.g., QC102, QC133, QC134, QC139, and QC143), which displayed lower *OsFTL1* expression and

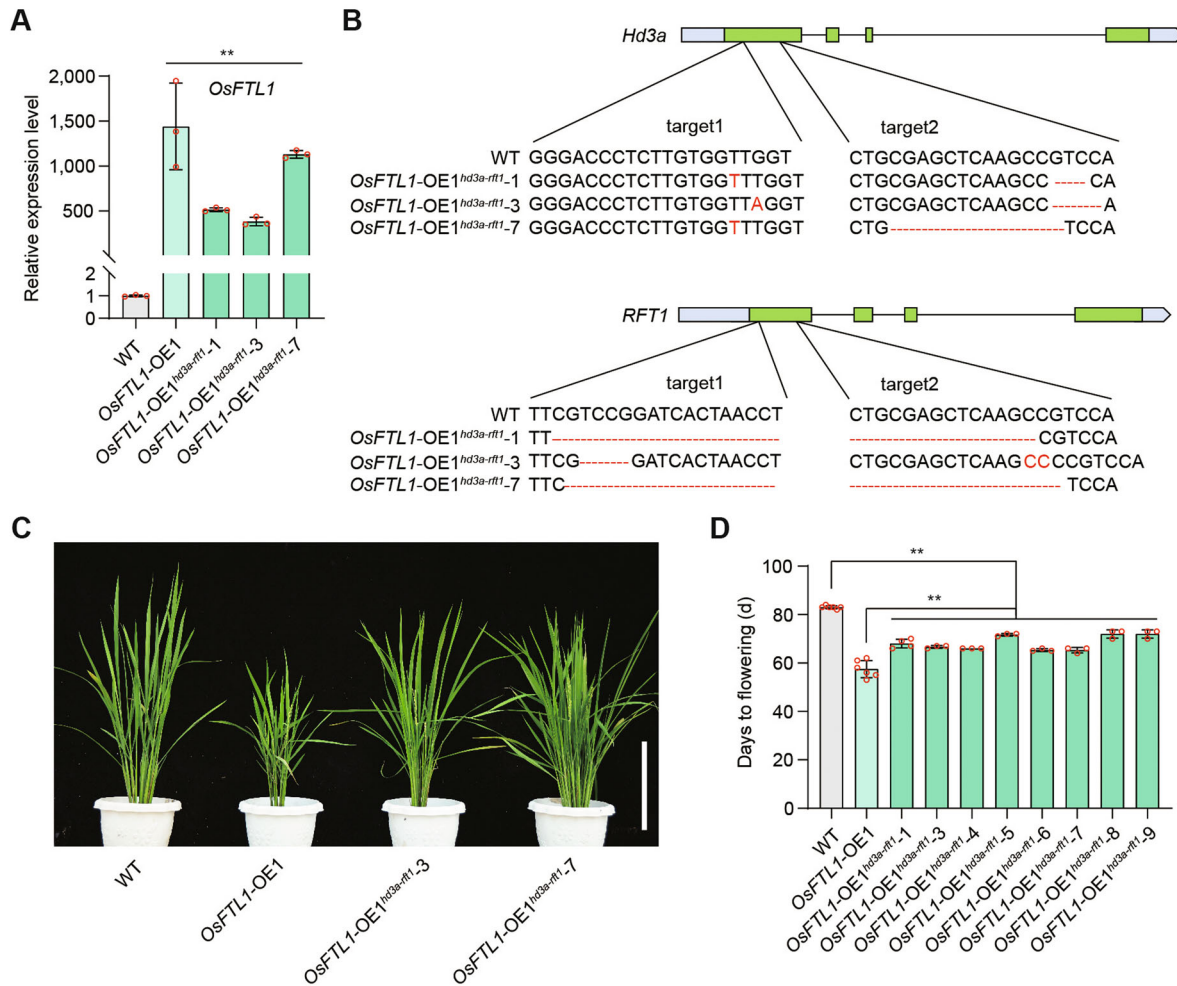


**Figure 6. *OsFTL1* promotes rice flowering without essential florigens *Hd3a* and *RFT1***

(A) Expression level of *OsFTL1* in the leaves of wild-type (WT), *OsFTL1-OE1*, *OsFTL1-OE1<sup>hd3a-rtt1</sup>* plants ( $n=3$  biological replicates). (B) Nucleotide sequences of *Hd3a* and *RFT1* targeted by CRISPR-Cas9 in WT and *OsFTL1-OE1<sup>hd3a-rtt1</sup>* plants. (C) Flowering phenotype of WT, *OsFTL1-OE1*, and *OsFTL1-OE1<sup>hd3a-rtt1</sup>* in Beijing in 2023, scale bar: 20 cm. (D) Flowering time of WT, *OsFTL1-OE1*, and *OsFTL1-OE1<sup>hd3a-rtt1</sup>* in Beijing in 2023 ( $n > 3$  biological replicates). \* and \*\* represent statistically significant differences compared with WT and *OsFTL1-OE1* at  $P < 0.05$  and  $P < 0.01$ , respectively, based on Student's *t*-tests.

later flowering (Figure S11A–C). Importantly, these differences in flowering time did not result in significant variations in grain yield across haplotypes (Figure S11D). Geographic analysis revealed that *OsFTL1-Hap3* was predominantly distributed in southern China (Figure 7G), suggesting that this haplotype could be particularly beneficial for breeding early-flowering rice varieties in high-latitude regions.

To investigate the evolutionary history of *OsFTL1*, we analyzed its gene region and 10-kb flanking regions in the rice micro-core germplasm. The 4-kb promoter region of *OsFTL1* underwent selection in both the *indica* and *japonica* subspecies, with the stronger selection pressure observed in the latter (Figure S12A). Nucleotide diversity ( $\pi$ ) values in the *OsFTL1* promoter decreased from 0.0179 in *Oryza rufipogon* to 0.0089 in *O. sativa indica* and 0.0046 in *O. sativa japonica* (Figure S12B), further indicating selective pressure on the *OsFTL1* promoter during domestication. In summary, our

findings suggested that elite *OsFTL1* alleles derived from *O. rufipogon* and *indica* subspecies represent valuable genetic resources for breeding early-maturing rice varieties.

## DISCUSSION

Flowering time in plants is determined by a combination of endogenous signals and environmental factors. Environmental cues are perceived in the leaves and transmitted to the SAM as molecular signals, primarily through florigens. These central flowering regulators promote the transition from vegetative to reproductive stages and play a crucial role in determining flowering time and yield-related traits. The function of florigens is highly conserved across the plant kingdom. Grafting experiments in various species, including tomato, tobacco, *Arabidopsis*, and rice, have demonstrated

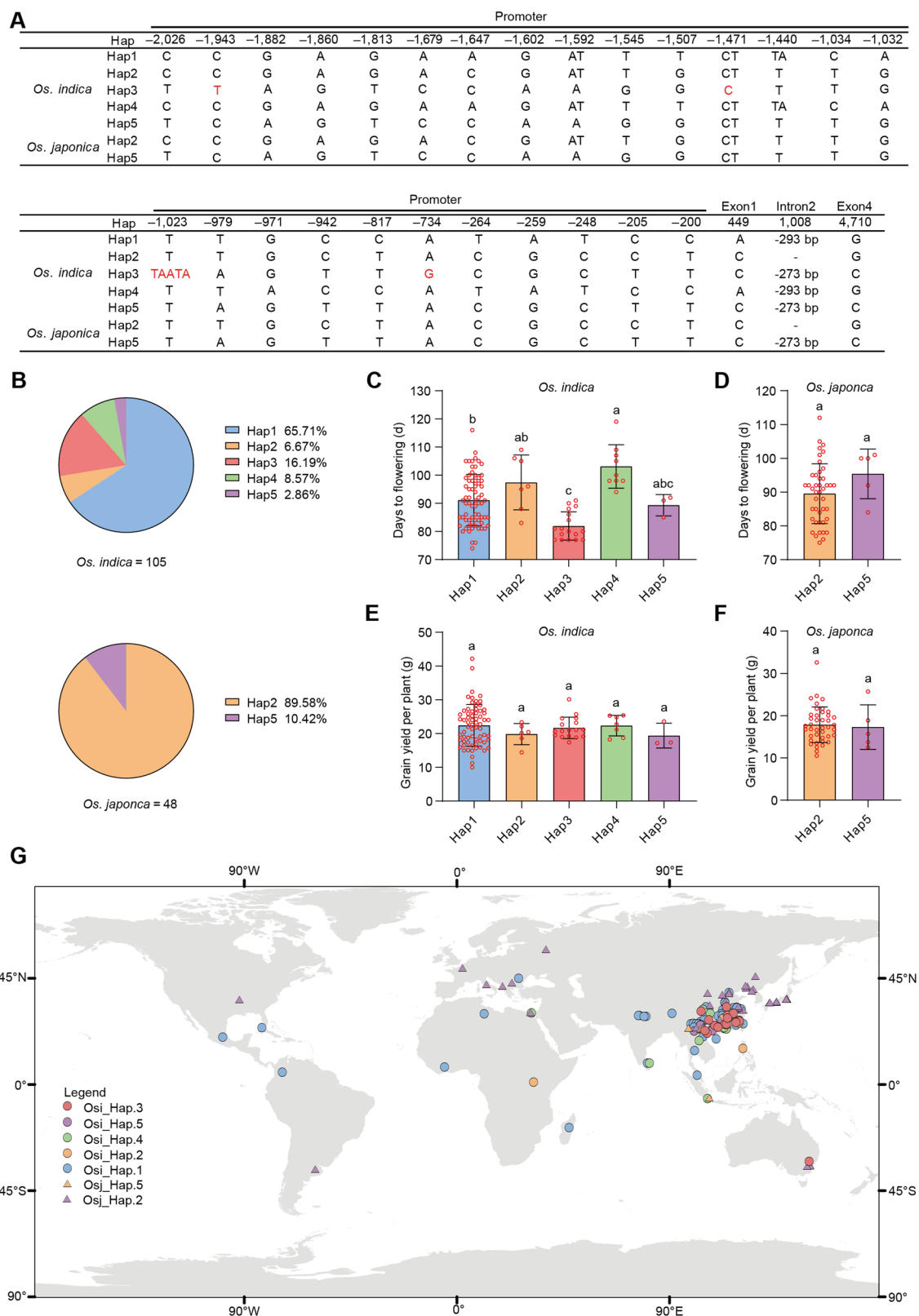


**Figure 7. Haplotypes and natural domestication of *OsFTL1***

(A) Haplotype analysis of polymorphisms in the promoter and gene body of *OsFTL1*. Red letters in *OsFTL1-Hap3* indicate the candidate functional variation sites. (B) Proportions of each *OsFTL1* haplotype in *japonica* and *indica* rice populations. (C, D) Flowering time of *OsFTL1* haplotypes in *indica* (C) and *japonica* (D) populations. Grain yield per plant of *OsFTL1* haplotypes in *indica* (E) and *japonica* (F) populations. Different lowercase letters denote significant differences ( $P < 0.05$ ) between *OsFTL1* haplotypes. (G) Geographic distribution of *OsFTL1* haplotypes globally.

that florigens synthesized in leaves are transported over long distances to the SAM, where they induce flowering (Huang et al., 2005; Lifschitz et al., 2006; Tamaki et al., 2007). For example, overexpression of the apple florigen *MdFT1* promotes flowering through interaction with *MdWRKY6*, which activates *AFL1* expression (Zuo et al., 2024). Similarly, the *CaFT-LIKE* gene in pepper (*Capsicum annuum*), homologous to tomato *SFT*, restores the late flowering phenotype of *sft* mutants when overexpressed in tomato (Borovsky et al., 2020). In maize, *ZCN8*, the sole flowering-promoting member of the *Zea centroradialis* gene family, is expressed in leaves and transported via the phloem to the SAM to promote flowering. Inhibition of *ZCN8* expression using microRNAs delays flowering (Lazakis et al., 2011; Meng et al., 2011). In wheat, *TaFT1* mediates photoperiod and vernalization signaling to regulate the heading stage, with FT-D1 forming a FAC with 14-3-3 A and FDL6 to promote early flowering by regulating downstream flowering genes (Li et al., 2024). In soybeans, *GmFT2a* and *GmFT5a* promote flowering under short-day conditions, enabling adaptation to diverse photoperiods (Kong et al., 2010). The regulation of flowering by *FT* genes is highly conserved across the plant kingdom, and most florigens regulate flowering time through the formation of FACs. This molecular regulatory mechanism is relatively conserved throughout the plant kingdom.

In rice, there are 13 FT-like proteins with diverse roles. *Hd3a* and *RFT1* are well characterized florigens that form FACs with GF14b/GF14c and OsFD1 to promote flowering under short-day and long-day conditions, respectively (Kojima et al., 2002; Komiya et al., 2008; Peng et al., 2021). Conversely, *OsFTL12* inhibits flowering by forming a FRC complex with GF14b and OsFD1 (Zheng et al., 2023). Overexpression of *OsFTL10* accelerates flowering, whereas knockout of *OsFTL4* also promotes flowering (Fang et al., 2019b; Gu et al., 2022). Despite these discoveries, the interactions among FT-like proteins and their binding partners remain poorly understood. Our study shows that *OsFTL1* overexpression significantly promotes flowering, forming a FAC with GF14c and OsFD1 (Figures 4, S9).

Beyond flowering time, rice FT-like proteins also influence agronomic traits such as tiller number, plant height, and grain yield. For instance, the FAC formed by *Hd3a* promotes lateral branching, increasing tiller numbers (Tsuji et al., 2015). Overexpression of *OsFTL10* decreases plant height and grain yield under short-day conditions (Fang et al., 2019b), while the early-flowering *ostf4* mutant exhibits semi-dwarf architecture and reduced grain yield due to fewer grains per panicle (Gu et al., 2022). Consistent with these findings, our study showed that *OsFTL1*-OE plants had three times more panicles per plant than the WT (Figure 1D), with reduced plant height and fewer grains per panicle, suggesting a role for FT-like proteins in shaping plant architecture and yield traits, potentially mediated by hormone regulation (Figure 1C–H) (Zhu et al., 2021).

Unlike *Hd3a* and *RFT1*, whose expression is induced in leaves and transported through the phloem to the SAM

*OsFTL1* promotes flowering without essential florigens

(Taoka et al., 2013), *OsFTL1* is predominantly expressed in the shoot base, stem, and inflorescence, particularly during the heading stage (Figures 3C–E, S5C, S6). This suggests that *OsFTL1* does not rely on long-distance transport from leaves to the SAM to promote flowering. However, when expressed in leaves under a specific promoter, *OsFTL1* still promoted early flowering in Xiushui134, indicating its potential mobility (Figures 5B, D, S6).

Previous studies have shown that FACs involving *Hd3a*/*RFT1*, *GF14b*/*GF14c*, and *OsFD1* regulate flowering by modulating the downstream genes *OsMADS14* and *OsMADS15* (Taoka et al., 2011; Brambilla et al., 2017). Our findings revealed that *OsFTL1* uses a similar mechanism to promote flowering, particularly in FAC formation and transcriptional regulation (Figures 4, S9). Notably, while both *Hd3a* and *OsFTL1* are induced under short-day conditions, only *RFT1* responded to long-day conditions (Figure S7) (Kojima et al., 2002; Komiya et al., 2009).

Previous studies have established that *Hd3a* and *RFT1* are pivotal florigens in rice, as evidenced by the severely delayed flowering phenotype of *Hd3a*-*RFT1* RNAi plants, which can fail to flower for up to 300 d (Komiya et al., 2008). In this study, we knocked out both *Hd3a* and *RFT1* in *OsFTL1*-OE plants and observed that the flowering time of *OsFTL1*-OE<sup>*hd3a-rft1*</sup> plants in Beijing ranged from 66 to 72 d. This flowering period was shorter than that of Nipponbare (WT, 83 d) but longer than for *OsFTL1*-OE plants (57.5 d) (Figure 6C, D). These findings indicated that *OsFTL1* alone was sufficient to promote flowering in the absence of *Hd3a* and *RFT1*, suggesting that *OsFTL1* acts as a key florigen-like gene downstream of *Hd3a* and *RFT1*. Interestingly, the later flowering of *OsFTL1*-OE<sup>*hd3a-rft1*</sup> plants compared with *OsFTL1*-OE demonstrated that *Hd3a* and *RFT1* further enhanced flowering even in the presence of *OsFTL1*. While *OsFTL1* can promote flowering independently, it cannot fully compensate for the functions of *Hd3a* and *RFT1*. Further genetic interaction studies among *Hd3a*, *RFT1*, and *OsFTL1* could provide valuable insights and strategies for creating early-flowering rice varieties through the combinatory manipulation of florigens.

The impact of FT-like proteins on yield traits has garnered increasing attention due to their dual importance in regulating rice grain yield and flowering time (Tsuji et al., 2015; Fang et al., 2019b; Gu et al., 2022; Zhao et al., 2024). We evaluated the yield traits of *OsFTL1*-OE plants driven by the *UBI* promoter and found a significant reduction in grain yield compared with WT. However, plants expressing *OsFTL1* under its native promoter (*pOsFTL1::OsFTL1-GFP*) exhibited much higher grain yields, comparable with WT (Table S3), and had an average flowering time of 69.78 d. This flowering time in Beijing was later than that of *OsFTL1*-OE plants (51.6 d) but earlier than the WT (117.25 d) (Figures 1A, B, 5A, C). These results demonstrated that *OsFTL1* overexpression under its native promoter achieved a better balance between grain yield and flowering time compared with the *UBI* promoter, highlighting the potential of *OsFTL1* for targeted genetic manipulation.

Natural genetic variation offers a valuable resource for breeding crops with desirable traits tailored to diverse agricultural needs and environmental conditions. Variations in flowering-time-regulating genes, such as *RFT1*, *DTH8*, *Ghd7*, and *Hd1*, have been studied extensively and utilized successfully in rice breeding (Xue et al., 2008; Takahashi et al., 2009; Yan et al., 2011; Dai et al., 2012; Ogiso-Tanaka et al., 2013; Zhao et al., 2015; Li et al., 2016; Xu et al., 2014). To assess the utility of *OsFTL1* in breeding, we investigated its natural variations and identified *OsFTL1-Hap3* as an early-flowering haplotype with relatively higher *OsFTL1* expression, predominantly in the *indica* subspecies. Plants with *OsFTL1-Hap3* displayed earlier flowering and grain yields comparable with other haplotypes, making *OsFTL1-Hap3* a promising candidate for early-maturing rice breeding. Leveraging advanced gene-editing technologies, manipulating functional variation sites in the *OsFTL1-Hap3* promoter presents an important target for improving rice traits. This approach paves the way for precision breeding, offering a practical solution for developing rice varieties optimized for diverse agricultural contexts.

## MATERIALS AND METHODS

### Plasmid construction and plant transformation

The coding sequence (CDS) of *OsFTL1* was amplified from Nipponbare cDNA and cloned into the pTCK303 vector to generate the *pUBI::OsFTL1* plasmid. A 1,995-bp promoter of *OsFTL1*, amplified from Nipponbare genomic DNA, and the *OsFTL1* CDS were inserted into the pBWA(V)HII vector to create the *pOsFTL1::OsFTL1-GFP* plasmid. The same promoter was cloned into the pEGProGUS vector to construct the *pOsFTL1::GUS* plasmid. To drive *OsFTL1* expression specifically in leaves, a 2,000-bp promoter of *RFT1* was amplified and inserted with the *OsFTL1* CDS into the pBWA(V)H vector, resulting in the *pRFT1::OsFTL1* plasmid. All plasmids, except *pRFT1::OsFTL1*, were transformed into Nipponbare via *Agrobacterium* strain EHA105, while *pRFT1::OsFTL1* was introduced into Xiushui134. *OsFTL1-OE1<sup>hd3a-rft1</sup>* mutants were created using CRISPR-Cas9 gene editing on the *OsFTL1-OE1* background.

### Plant growth conditions

Field experiments were conducted in paddy fields in Beijing (natural long-day conditions) and Sanya (natural short-day conditions). Sowing times in Beijing in 2021, 2022, and 2024 were on May 16, May 30, and June 4, respectively. Seedlings were transplanted with 23.3 cm row spacing and 16.7 cm plant spacing. For photoperiod treatments, two greenhouses with identical environments but differing day lengths (16 h light/8 h dark for long days and 8 h light/16 h dark for short days) were used.

### Analysis of agronomic and physiological traits

Agronomic traits, including heading date, plant height, stem node number and length, stem diameter, leaf number, grain

number per panicle, tiller number, aboveground dry weight, grain weight, and grain yield per plant, were measured in the Beijing and Sanya field experiments. The flowering time (days to flowering) was recorded as the number of days from sowing to flowering.

### Quantitative real-time polymerase chain reaction analysis

Total RNA was extracted using a Total RNA Isolation Kit (Vazyme Biotech Co., Ltd.) and quantified with a NanoDrop 2000 spectrophotometer. cDNA synthesis was performed with 1 µg RNA treated with DNase I using the HiScript IV First Strand cDNA Synthesis Kit (Vazyme Biotech Co., Ltd., Nanjing, China). qPCR was conducted using Taq Pro Universal SYBR qPCR Master Mix (Vazyme Biotech Co., Ltd., Nanjing, China) on an ABI QuantStudio 6 Flex system. *OsActin* (*LOC\_Os03g50885*) was the internal control, and gene expression levels were calculated using the  $2^{-\Delta\Delta CT}$  method with three biological replicates. Primer sequences are listed in Table S4.

### RNA-seq and data analysis

Total RNA was extracted from 30-d-old *OsFTL1-OE1* and WT seedlings under long-day conditions using TRIzol reagent. RNA integrity was assessed with an Agilent 2100 Bioanalyzer, and libraries were prepared using a TruSeq Stranded mRNA LT Sample Prep Kit (Illumina, San Diego, USA). Sequencing was performed on an Illumina HiSeq X Ten platform, generating ~15 Gbp clean reads per sample. Reads were mapped to the Nipponbare reference genome using HISAT and Bowtie 2; gene expression was quantified in fragments per kilobase per million mapped fragments (FPKM) using Cufflinks. Differential expression analysis was performed with DESeq, with significance thresholds of  $P < 0.05$  and  $|\log_2 \text{fold change}| > 1$ . Heatmaps were generated using FPKM values via an online tool (<https://cloud.oebiotech.cn/task/>).

### Subcellular localization

The *OsFTL1* CDS was cloned into the pAN580 vector to fuse GFP at the C-terminus, while *GF14c* and *OsFD1* CDSs were fused with red fluorescent protein (RFP) in the pSAT6 vector. Constructs were transformed into rice protoplasts along with the *Ghd7-mCherry* nuclear marker for localization studies. Fluorescence was observed using a Zeiss LSM 980 confocal microscope. Primers are listed in Table S4.

### Phylogenetic tree

A phylogenetic tree was constructed using 13 FTL protein sequences from the Rice Annotation Project Database (<https://rapdb.dna.affrc.go.jp/>) and three FTL1 sequences from the National Center for Biotechnology Information (<https://blast.ncbi.nlm.nih.gov/Blast.cgi>). The evolutionary history was inferred using the maximum likelihood method with the JTT matrix-based model in MEGA (version 7; <https://www.megasoftware.net>). Bootstrap values were estimated (with 1,000 replicates) to evaluate the relative support, and bootstrap values of 50% and higher are shown on the tree.

### GUS staining assay

Tissues from *pOsFTL1::GUS* plants and WT were incubated in GUS staining buffer (GUSBlue Kit, Huayueyang, Beijing, China) at 37°C overnight. Chlorophyll was removed with 70% ethanol, and samples were imaged using an Olympus BX53 microscope and a Zeiss SteREO Discovery.V8 stereoscope.

### Immunoblot assay

Total protein was extracted from shoot base, leaf, leaf sheath, and glume of *pOsFTL1::OsFTL1-GFP* plants in 200  $\mu$ L of extraction buffer containing 20 mM Tris (pH 7.5), 100 mM NaCl, 2.5 mM MgCl<sub>2</sub>, 1 mM EGTA, 1 mM DTT, and protease inhibitor cocktail (1:50; Roche, Basel, Switzerland). After quantification and denaturation, 20  $\mu$ g of protein were separated by SDS-PAGE and transferred to PVDF membranes (GE Healthcare, Chicago, USA). After blocking with 5% skimmed milk in TBST buffer (20 mM Tris/HCl, pH 7.6, 137 mM NaCl, 0.1% Tween) at 4°C overnight, membranes were incubated with primary antibodies against GFP (11814460001; Roche, Basel, Switzerland), Flag (F1804; Sigma-Aldrich, St. Louis, USA), GST (SAB4200237; Sigma-Aldrich, St. Louis, USA), and His (SAB2702218; Sigma-Aldrich, St. Louis, USA) at dilutions recommended by the manufacturers, followed by incubation with secondary antibody (anti-mouse IgG, A9044; Sigma-Aldrich, St. Louis, USA) at a 1:20,000 dilution. Membranes were imaged using a chemiluminescence imaging device (Celvin S, Biostep, Jarville-la-Malgrange, France) after incubation in ECL solution (GE Healthcare, Chicago, USA) for 5 min at room temperature.

### Immunoprecipitation-MS

Immunoprecipitation-MS was performed following the instructions provided with a  $\mu$ MACS Epitope Tag Protein Isolation Kit (130091125; Miltenyi Biotec, Bergisch Gladbach, Germany). One gram of *pUBI::OsFTL1-GFP* and WT plant seedlings were ground in a mortar. Protein extraction, Co-IP, and elution were conducted according to the manufacturer's protocol. Proteins in the elution buffer were analyzed via SDS-PAGE and a Q Exactive mass spectrometer. The MS raw data for each sample were integrated and searched using MaxQuant software for identification and quantitation.

### Bimolecular fluorescence complementation

The CDSs of *OsFTL1* and *GF14c* were cloned into p2YN-YFP and p2YC-cYFP vectors, respectively. Constructs were introduced into *Nicotiana benthamiana* leaves via *Agrobacterium*-mediated transformation using strain GV3101. The CDSs of *OsFTL1* and *GF14c* also were cloned into VN-cYFP and VC-cYFP vectors, respectively. Constructs were introduced into rice protoplasts. Yellow fluorescent protein (YFP) fluorescence was observed 48 h post-infiltration using a Zeiss LSM 980 confocal laser scanning microscope.

### Co-immunoprecipitation

The CDSs of *OsFTL1* and *GF14c* were cloned into pAN580-GFP and pAN580-Flag vectors to create *p35S::OsFTL1-GFP* and *p35S::GF14c-Flag* plasmids. These constructs were transformed into rice protoplasts and incubated overnight.

*OsFTL1* promotes flowering without essential florigens

Proteins were extracted in protein extraction buffer, incubated with GFP beads (D153-11; MBL, Darmstadt, Germany) at 4°C for 1 h, washed with wash buffer, and analyzed by SDS-PAGE. Immunoblotting was performed using anti-GFP (11814460001; Roche, Basel, Switzerland) and anti-Flag (F1804; Sigma-Aldrich, St. Louis, USA) monoclonal antibodies.

### Pull-down assay

The CDSs of *OsFTL1* and *GF14c* were cloned into pGEX-4T-1 and pCZN1 vectors to express recombinant GST-*OsFTL1* and *GF14c*-His fusion proteins in *Escherichia coli* BL21 (TSC-E06; Tsingke, Beijing, China). The pull-down assay was performed as described (Miernyk and Thelen, 2008), and proteins were detected with anti-GST (AG8054; Beyotime, Shanghai, China) and anti-His (10010; Zomanbio, Beijing, China) antibodies at 1:2,000 dilution.

### Dual-luciferase transcriptional activity assay

Effector plasmids pAN580-*OsFTL1*, pSAT6-*GF14c*, pSAT6-*OsFD1*, and empty pAN580 were used alongside reporter plasmids constructed by cloning ~2-kb promoter regions of *OsMADS14* and *OsMADS15* into pGREEN II 0800. These were co-transformed into rice protoplasts, incubated in the dark at 28°C for 16 h, and analyzed using a Dual-Luciferase Reporter Assay System Kit (E1910; Promega, Wisconsin, USA) and TriStar2 Multimode Reader LB942 (Berthold Technologies). The Renilla luciferase gene under the CaMV 35S promoter served as an internal control. Primer sequences are listed in Table S4.

### Haplotype and nucleotide diversity analysis

Haplotype analysis was performed using gene and 2-kb upstream promoter variant data, including SNPs, indels, and structural variations. Super pan-genomic variant data (Shang et al., 2022) and the complete *Oryza sativa* cv. Nipponbare genome (Shang et al., 2023) served as the data source. Variants were filtered using VCFtools (v0.1.16) with an allele frequency  $\geq 0.05$  and maximum missing rate  $\leq 0.1$ . The promoter region analysis included all variants, whereas the gene region focused on non-synonymous mutations. Phenotypic differences among haplotypes were assessed by Duncan's multiple range test using GraphPad Prism (v9.5). Nucleotide diversities ( $\pi$ ) were calculated using a 500-bp window and 100-bp step size with VCFtools, covering 10-kb flanking regions of *OsFTL1* (Danecek et al., 2011; Shang et al., 2022).

### Statistical analysis

Significant differences were assessed using a two-tailed Student's *t*-test in Microsoft® Excel 2010. Results with a *P*-value  $< 0.05$  were considered statistically significant. Figures were prepared using GraphPad Prism (v7.0 and v9.0) and R software (v3.6.1).

### Data availability statement

The raw RNA-seq data supporting this study were deposited in the NCBI Sequence Read Archive under accession number PRJNA1116605.

## ACKNOWLEDGEMENTS

This research was supported by grants from the Key Program of National Natural Science Foundation of China (32330079), the STI 2030-Major Projects (2023ZD0407203), the Innovation Program of Chinese Academy of Agricultural Sciences, the Nanfan Special Project of CAAS (YBXM02), the China Postdoctoral Science Foundation (2023M743846) and the Youth Program of National Natural Science Foundation of China (32401746).

## CONFLICTS OF INTEREST

The authors declare no conflict of interest.

## AUTHOR CONTRIBUTIONS

W.Z., Q.Q., and S.W. designed the experiments. S.W., and Lo.C. performed most of the experiments and data analyses. H.Q. performed the haplotype and nucleotide diversity analysis. L.S. shared the rice micro-core germplasm resources and related data. Yuj.Z., X.Y., Yup.Z., Y.G., L.C., and C.X. performed field trials and data analyses. S.W. wrote the manuscript. W.Z., Q.Q., and X.L. revised the manuscript. All authors read and approved the content of this paper.

**Edited by:** Young Hun Song, Seoul National University, Korea

**Received** Dec. 5, 2024; **Accepted** Jan. 11, 2025

## REFERENCES

- Borovsky, Y., Mohan, V., Shabtai, S., and Paran, I.** (2020). CaFT-LIKE is a flowering promoter in pepper and functions as florigen in tomato. *Plant Sci.* **301**: 110678.
- Brambilla, V., Martignago, D., Goretti, D., Cerise, M., Somssich, M., de Rosa, M., Galbiati, F., Shrestha, R., Lazzaro, F., Simon, R., et al.** (2017). Antagonistic transcription factor complexes modulate the floral transition in rice. *Plant Cell* **29**: 2801–2816.
- Cho, L., Yoon, J., Pasriga, R., and An, G.** (2016). Homodimerization of Ehd1 is required to induce flowering in rice. *Plant Physiol.* **170**: 2159–2171.
- Cho, L.H., Yoon, J., and An, G.** (2017). The control of flowering time by environmental factors. *Plant J.* **90**: 708–719.
- Dai, X., Ding, Y., Tan, L., Fu, Y., Liu, F., Zhu, Z., Sun, X., Sun, X., Gu, P., Cai, H., et al.** (2012). *LHD1*, an allele of *DTH8/Ghd8*, controls late heading date in common wild rice (*Oryza rufipogon*). *J. Integr. Plant Biol.* **54**: 790–799.
- Danecek, P., Auton, A., Abecasis, G., Albers, C., Banks, E., DePristo, M., Handsaker, R., Lunter, G., Marth, G.T., Sherry, S.T., et al.** (2011). The variant call format and VCFtools. *Bioinformatics* **27**: 2156–2158.
- Doi, K., Izawa, T., Fuse, T., Yamanouchi, U., Kubo, T., Shimatani, Z., Yano, M., and Yoshimura, A.** (2004). *Ehd1*, a B-type response regulator in rice, confers short-day promotion of flowering and controls *FT*-like gene expression independently of *Hd1*. *Genes Dev.* **18**: 926–936.
- Fang, J., Zhang, F., Wang, H., Wang, W., Zhao, F., Li, Z., Sun, C., Chen, F., Xu, F., Chang, S., et al.** (2019a). *Ef-cd* locus shortens rice maturity

duration without yield penalty. *Proc. Natl. Acad. Sci. U.S.A.* **116**: 18717–18722.

- Fang, M., Zhou, Z., Zhou, X., Yang, H., Li, M., and Li, H.** (2019b). Overexpression of *OsFTL10* induces early flowering and improves drought tolerance in *Oryza sativa* L. *PeerJ* **7**: e6422.
- Giaume, F., Bono, G.A., Martignago, D., Miao, Y., Vicentini, G., Toriba, T., Wang, R., Kong, D., Cerise, M., Chirivi, D., et al.** (2023). Two florigens and a florigen-like protein form a triple regulatory module at the shoot apical meristem to promote reproductive transitions in rice. *Nat. Plants.* **9**: 525–534.
- Gu, H., Zhang, K., Chen, J., Gull, S., Chen, C., Hou, Y., Li, X., Miao, J., Zhou, Y., and Liang, G.** (2022). *OsFTL4*, an *FT*-like gene, regulates flowering time and drought tolerance in rice (*Oryza sativa* L.). *Rice* **15**: 47.
- Huang, T., Böhlenius, H., Eriksson, S., Parcy, F., and Nilsson, O.** (2005). The mRNA of the Arabidopsis gene *FT* moves from leaf to shoot apex and induces flowering. *Science* **309**: 1694–1696.
- Izawa, T., Oikawa, T., Sugiyama, N., Tanisaka, T., Yano, M., and Shimamoto, K.** (2002). Phytochrome mediates the external light signal to repress *FT* orthologs in photoperiodic flowering of rice. *Genes Dev.* **16**: 2006–2020.
- Jin, S., Nasim, Z., Susila, H., and Ahn, J.** (2021). Evolution and functional diversification of *FLOWERING LOCUS T/TERMINAL FLOWER 1* family genes in plants. *Semin. Cell Dev. Biol.* **109**: 20–30.
- Kim, S., Lee, S., Kim, H., Nam, H., and An, G.** (2007). *OsMADS51* is a short-day flowering promoter that functions upstream of *Ehd1*, *OsMADS14*, and *Hd3a*. *Plant Physiol.* **145**: 1484–1494.
- Kojima, S., Takahashi, Y., Kobayashi, Y., Monna, L., Sasaki, T., Araki, T., and Yano, M.** (2002). *Hd3a*, a rice ortholog of the Arabidopsis *FT* gene, promotes transition to flowering downstream of *Hd1* under short-day conditions. *Plant Cell Physiol.* **43**: 1096–1105.
- Komiya, R., Ikegami, A., Tamaki, S., Yokoi, S., and Shimamoto, K.** (2008). *Hd3a* and *RFT1* are essential for flowering in rice. *Development* **135**: 767–774.
- Komiya, R., Yokoi, S., and Shimamoto, K.** (2009). A gene network for long-day flowering activates *RFT1* encoding a mobile flowering signal in rice. *Development* **136**: 3443–3450.
- Kong, F., Liu, B., Xia, Z., Sato, S., Kim, B.M., Watanabe, S., Yamada, T., Tabata, S., Kanazawa, A., Harada, K., et al.** (2010). Two coordinately regulated homologs of *FLOWERING LOCUS T* are involved in the control of photoperiodic flowering in soybean. *Plant Physiol.* **154**: 1220–1231.
- Lazakis, C.M., Coneva, V., and Colasanti, J.** (2011). *ZCN8* encodes a potential orthologue of Arabidopsis *FT* florigen that integrates both endogenous and photoperiod flowering signals in maize. *J. Exp. Bot.* **62**: 4833–4842.
- Lee, S., Kim, J., Han, J., Han, M., and An, H.** (2004). Functional analyses of the flowering time gene *OsMADS50*, the putative *SUPPRESSOR OF OVEREXPRESSION OF CO 1/AGAMOUS-LIKE 20 (SOC1/AGL20)* ortholog in rice. *Plant J.* **38**: 754–764.
- Lee, Y., Jeong, D., Lee, D., Yi, J., Ryu, C., Kim, S., Jeong, H., Choi, S., Jin, P., Yang, J., et al.** (2010). *OsCOL4* is a constitutive flowering repressor upstream of *Ehd1* and downstream of *OsphyB*. *Plant J.* **63**: 18–30.
- Li, Q., Yan, W., Chen, H., Tan, C., Han, Z., Yao, W., Li, G., Yuan, M., and Xing, Y.** (2016). Duplication of *OsHAP* family genes and their association with heading date in rice. *J. Exp. Bot.* **67**: 1759–1768.
- Li, Y., Xiong, H., Guo, H., Xie, Y., Zhao, L., Gu, J., Li, H., Zhao, S., Ding, Y., Zhou, C., et al.** (2024). A gain-of-function mutation at the C-terminus of *FT-D1* promotes heading by interacting with 14-3-3A and FDL6 in wheat. *Plant Biotechnol. J.* **23**: 20–35.
- Lifschitz, E., Eviatar, T., Rozman, A., Shalit, A., Goldshmidt, A., Amshel, Z., Alvarez, J.P., and Eshed, Y.** (2006). The tomato *FT*

- ortholog triggers systemic signals that regulate growth and flowering and substitute for diverse environmental stimuli. *Proc. Natl. Acad. Sci. U.S.A.* **103**: 6398–6403.
- Liu, L., Zhang, Y., Yang, Z.F., Yang, Q., Zhang, Y., Xu, P., Li, J., Islam, A., Shah, L., Zhan, X.D., et al. (2022). Fine mapping and candidate gene analysis of *qHD1b*, a QTL that promotes flowering in common wild rice (*Oryza rufipogon*) by up-regulating *Ehd1*. *Crop J.* **10**: 1083–1093.
- Matsubara, K., Yamanouchi, U., Wang, Z., Minobe, Y., Izawa, T., and Yano, M. (2008). *Ehd2*, a rice ortholog of the maize *INDETERMINATE1* gene, promotes flowering by up-regulating *Ehd1*. *Plant Physiol.* **148**: 1425–1435.
- Meng, X., Muszynski, M.G., and Danilevskaia, O.N. (2011). The *FT-like* ZCN8 gene functions as a floral activator and is involved in photoperiod sensitivity in maize. *Plant Cell* **23**: 942–960.
- Miernyk, J.A., and Thelen, J.J. (2008). Biochemical approaches for discovering protein-protein interactions. *Plant J.* **53**: 597–609.
- Ogiso-Tanaka, E., Matsubara, K., Yamamoto, S., Nonoue, Y., Wu, J., Fujisawa, H., Ishikubo, H., Tanaka, T., Ando, T., Matsumoto, T., et al. (2013). Natural variation of the *RICE FLOWERING LOCUS T 1* contributes to flowering time divergence in rice. *PLoS One* **8**: e75959.
- Peng, Q., Zhu, C., Liu, T., Zhang, S., Feng, S., and Wu, C. (2021). Phosphorylation of OsFD1 by OsCIPK3 promotes the formation of RFT1-containing florigen activation complex for long-day flowering in rice. *Mol. Plant* **14**: 1135–1148.
- Shang, L., He, W., Wang, T., Yang, Y., Xu, Q., Zhao, X., Yang, L., Zhang, H., Li, X., Lv, Y., et al. (2023). A complete assembly of the rice Nipponbare reference genome. *Mol. Plant* **16**: 1232–1236.
- Shang, L., Li, X., He, H., Yuan, Q., Song, Y., Wei, Z., Lin, H., Hu, M., Zhao, F., Zhang, C., et al. (2022). A super pan-genomic landscape of rice. *Cell Res.* **32**: 878–896.
- Sheng, P., Wu, F., Tan, J., Zhang, H., Ma, W., Chen, L., Wang, J., Wang, J., Zhu, S., Guo, X., et al. (2016). A *CONSTANS-like* transcriptional activator, *OsCOL13*, functions as a negative regulator of flowering downstream of *OsphyB* and upstream of *Ehd1* in rice. *Plant Mol. Biol.* **92**: 209–222.
- Song, S., Chen, Y., Liu, L., Wang, Y., Bao, S., Zhou, X., Teo, Z., Mao, C., Gan, Y., and Yu, H. (2017). OsFTIP1-mediated regulation of florigen transport in rice is negatively regulated by the Ubiquitin-like domain kinase OsUbdKγ4. *Plant Cell* **29**: 491–507.
- Sun, C., Chen, D., Fang, J., Wang, P., Deng, X., and Chu, C. (2014). Understanding the genetic and epigenetic architecture in complex network of rice flowering pathways. *Protein Cell* **5**: 889–898.
- Takahashi, Y., Teshima, K., Yokoi, S., Innan, H., and Shimamoto, K. (2009). Variations in *Hd1* proteins, *Hd3a* promoters, and *Ehd1* expression levels contribute to diversity of flowering time in cultivated rice. *Proc. Natl. Acad. Sci. U.S.A.* **106**: 4555–4560.
- Tamaki, S., Matsuo, S., Wong, H., Yokoi, S., and Shimamoto, K. (2007). Hd3a protein is a mobile flowering signal in rice. *Science* **316**: 1033–1036.
- Taoka, K., Ohki, I., Tsuji, H., Furuita, K., Hayashi, K., Yanase, T., Yamaguchi, M., Nakashima, C., Purwestri, Y., Tamaki, S., et al. (2011). 14-3-3 proteins act as intracellular receptors for rice Hd3a florigen. *Nature* **476**: 332–335.
- Taoka, K., Ohki, I., Tsuji, H., Kojima, C., and Shimamoto, K. (2013). Structure and function of florigen and the receptor complex. *Trends Plant Sci.* **18**: 287–294.
- Tsuji, H., Tachibana, C., Tamaki, S., Taoka, K., Kyozuka, J., and Shimamoto, K. (2015). Hd3a promotes lateral branching in rice. *Plant J.* **82**: 256–266.
- Vicentini, G., Biancucci, M., Minerì, L., Chirivì, D., Giaume, F., Miao, Y., Kyozuka, J., Brambilla, V., Betti, C., and Fornara, F. (2023). Environmental control of rice flowering time. *Plant Commun.* **4**: 100610.
- OsFTL1 promotes flowering without essential florigens
- Wang, P., Zhou, G., Yu, H., and Yu, S. (2011). Fine mapping a major QTL for flag leaf size and yield-related traits in rice. *Theor. Appl. Genet.* **123**: 1319–1330.
- Wei, S., Li, X., Lu, Z., Zhang, H., Ye, X., Zhou, Y., Li, J., Yan, Y., Pei, H., Duan, F., et al. (2022). A transcriptional regulator that boosts grain yields and shortens the growth duration of rice. *Science* **377**: eabi8455.
- Wei, X., Chen, M., Zhang, Q., Gong, J., Liu, J., Yong, K., Wang, Q., Fan, J., Chen, S., Hua, H., et al. (2024). Genomic investigation of 18,421 lines reveals the genetic architecture of rice. *Science* **385**: eadm8762.
- Wei, X., Xu, J., Guo, H., Jiang, L., Chen, S., Yu, C., Zhou, Z., Hu, P., Zhai, H., and Wan, J. (2010). *DTH8* suppresses flowering in rice, influencing plant height and yield potential simultaneously. *Plant Physiol.* **153**: 1747–1758.
- Xu, Q., Saito, H., Hirose, I., Katsura, K., Yoshitake, Y., Yokoo, T., Tsukiyama, T., Teraishi, M., Tanisaka, T., and Okumoto, Y. (2014). The effects of the photoperiod-insensitive alleles, *se13*, *hd1* and *ghd7*, on yield components in rice. *Mol. Breed.* **33**: 813–819.
- Xue, W., Xing, Y., Weng, X., Zhao, Y., Tang, W., Wang, L., Zhou, H., Yu, S., Xu, C., Li, X., et al. (2008). Natural variation in *Ghd7* is an important regulator of heading date and yield potential in rice. *Nat. Genet.* **40**: 761–767.
- Yan, W., Wang, P., Chen, H., Zhou, H., Li, Q., Wang, C., Ding, Z., Zhang, Y., Yu, S., Xing, Y., et al. (2011). A major QTL, *Ghd8*, plays pleiotropic roles in regulating grain productivity, plant height, and heading date in rice. *Mol. Plant* **4**: 319–330.
- Yano, M., Katayose, Y., Ashikari, M., Yamanouchi, U., Monna, L., Fuse, T., Baba, T., Yamamoto, K., Umehara, Y., Nagamura, Y., et al. (2000). *Hd1*, a major photoperiod sensitivity quantitative trait locus in rice, is closely related to the Arabidopsis flowering time gene *CONSTANS*. *Plant Cell* **12**: 2473–2484.
- Zhang, L., Zhang, F., Zhou, X., Poh, T., Xie, L., Shen, J., Yang, L., Song, S., Yu, H., and Chen, Y. (2022). The tetratricopeptide repeat protein OsTPR075 promotes heading by regulating florigen transport in rice. *Plant Cell* **34**: 3632–3646.
- Zhao, H., Shan, J., Ye, W., Dong, N., Kan, Y., Yang, Y., Yu, H., Lu, Z., Guo, S., Lei, J., et al. (2024). A QTL *GN1.1*, encoding FT-L1, regulates grain number and yield by modulating polar auxin transport in rice. *J. Integr. Plant Biol.* **66**: 2158–2174.
- Zhao, J., Chen, H., Ren, D., Tang, H., Qiu, R., Feng, J., Long, Y., Niu, B., Chen, D., Zhong, T., et al. (2015). Genetic interactions between diverged alleles of *Early heading date 1* (*Ehd1*) and *Heading date 3a* (*Hd3a*)/*RICE FLOWERING LOCUS T1* (*RFT1*) control differential heading and contribute to regional adaptation in rice (*Oryza sativa*). *New Phytol.* **208**: 936–948.
- Zheng, R., Meng, X., Hu, Q., Yang, B., Cui, G., Li, Y., Zhang, S., Zhang, Y., Ma, X., Song, X., et al. (2023). OsFTL12, a member of FT-like family, modulates the heading date and plant architecture by florigen repression complex in rice. *Plant Biotechnol. J.* **21**: 1343–1360.
- Zhou, S., Zhu, S., Cui, S., Hou, H., Wu, H., Hao, B., Cai, L., Xu, Z., Liu, L., Jiang, L., et al. (2021). Transcriptional and post-transcriptional regulation of heading date in rice. *New Phytol.* **230**: 943–956.
- Zhu, Y., Klasfeld, S., and Wagner, D. (2021). Molecular regulation of plant developmental transitions and plant architecture via PEPB family proteins: An update on mechanism of action. *J. Exp. Bot.* **72**: 2301–2311.
- Zong, W., Ren, D., Huang, M., Sun, K., Feng, J., Zhao, J., Xiao, D., Xie, W., Liu, S., Zhang, H., et al. (2021). Strong photoperiod sensitivity is controlled by cooperation and competition among *Hd1*, *Ghd7* and *DTH8* in rice heading. *New Phytol.* **229**: 1635–1649.
- Zuo, X., Wang, S., Liu, X., Tang, T., Li, Y., Tong, L., Shah, K., Ma, J., An, N., Zhao, C., et al. (2024). FLOWERING LOCUS T1 and TERMINAL FLOWER1 regulatory networks mediate flowering initiation in apple. *Plant Physiol.* **195**: 580–597.

**SUPPORTING INFORMATION**

Additional Supporting Information may be found online in the supporting information tab for this article: <http://onlinelibrary.wiley.com/doi/10.1111/jipb.13856/supinfo>

**Figure S1.** Expression level of *OsFTL1* in the leaves of *OsFTL1*-overexpressing (*OsFTL1*-OE) lines and wild-type (WT; cv. Nipponbare)

**Figure S2.** Grain phenotype of *OsFTL1*-OE plants and wild-type (WT) in Beijing in 2024

**Figure S3.** Stem characteristics of *OsFTL1*-OE and wild-type (WT)

**Figure S4.** Overexpression of *OsFTL1* were insensitive to day length

**Figure S5.** The expression of *OsFTL1* is more abundant under short-day conditions

**Figure S6.** Laser confocal microscopy observation of *OsFTL1*-GFP protein in the shoot apical meristem of *pOsFTL1::OsFTL1-GFP* plants

**Figure S7.** Expression analysis of florigen genes in different developmental stages of 9311 and Nipponbare

**Figure S8.** The interaction between *OsFTL1* and GF14c in rice protoplasts in bimolecular fluorescence complementation (BiFC) assay

**Figure S9.** Expression levels of flowering genes in *OsFTL1*-OE1 and wild-type (WT) under natural long-day conditions in Beijing

**Figure S10.** Flowering time of *OsFTL1*-OE *hd3a-fft1* and *hd3a-fft1* double knockout plants in Beijing in 2024

**Figure S11.** Agronomic traits of early flowering *OsFTL1*-Hap3 and other haplotypes

**Figure S12.** Nucleotide diversity analysis in *OsFTL1*

**Figure S13.** A proposed working model of *OsFTL1* promoting rice flowering

**Table S1.** Agronomic traits of *OsFTL1*-OE and wild-type (WT) in Beijing in 2021

**Table S2.** Candidate proteins interacting with *OsFTL1* by IP-MS

**Table S3.** Grain yield of *OsFTL1*-OE, *pOsFTL1::OsFTL1-GFP* and wild-type (WT) in Beijing in 2023

**Table S4.** Primers used in this research



Scan the QR code to view JIPB on WeChat  
(WeChat: [jipb1952](#))



Scan the QR code to view JIPB on Twitter  
(Twitter: [@JIPBio](#))